Research Square

Preprints are preliminary reports that have not undergone peer review.
They should not be considered conclusive, used to inform clinical practice,
or referenced by the media as validated information.

Synthesis of bundle copolymers as an emergent class of copolymer architecture

Takashi Uemura

uemurat@g.ecc.u-tokyo.ac.jp

The University of Tokyo https://orcid.org/0000-0002-1357-3196

Yuki Kametani

Institute of Engineering Innovation, School of Engineering, The University of Tokyo
https://orcid.org/0000-0002-1853-4110

Rintaro Yamaguchi

The University of Tokyo

Yusuke Ando

The University of Tokyo

Yuta Kawasaki

The University of Tokyo

Article

Keywords:

Posted Date: October 21st, 2025

DOI: https://doi.org/10.21203/rs.3.rs-7756650/v1

License: This work is licensed under a Creative Commons Attribution 4.0 International License.
Read Full License

Additional Declarations: There is **NO** Competing Interest.

Version of Record: A version of this preprint was published at Nature Communications on June 10th, 2026. See the published version at https://doi.org/10.1038/s41467-026-73978-1.

Abstract

Copolymers play a central role in soft materials owing to their capacity for diverse molecular designs. While numerous combinations of composition and topology have been explored for the development of copolymers, only four types of basic architecture (random, sequence-controlled, block, and graft) have been synthetically and historically achievable. Herein, we introduce a new class of copolymers—*bundle copolymers*—comprising multiple different chains interlinked and aligned in a parallel configuration. To exemplify this concept, bundle copolymers are synthesised via nanoconfined polymerisation, in which radical polymerisation of vinyl monomers occurs alongside vinyl-functionalised polydimethylsiloxane within the one-dimensional channels of a metal–organic framework. Unlike conventional copolymers, bundle copolymers feature aligned lateral strands whose proximity can be modulated by the density of covalent junctions. This innovative approach for tying multiple chains opens a new avenue for copolymer design, expanding the landscape of polymer chemistry.

Introduction

Copolymers, formed by combining different monomer units, are a central class of macromolecules with widespread importance in materials science and polymer chemistry. Their capacity to introduce molecular diversity often imparts properties inaccessible to homopolymers, rendering them indispensable in both fundamental research and industrial applications[1–4]. In 1994, the International Union of Pure and Applied Chemistry (IUPAC) formally classified copolymers into four primary categories based on the arrangement of monomer units: random (statistical), sequence-controlled (alternating, periodic), block, and graft (Fig. 1a)[5]. These established types and their combinations have provided an outline for the rational design of functional copolymer materials. Over the past decades, advances in polymer synthesis have enabled precise control over these architectures[6–11], demonstrating that both chemical composition and structural design play a key role in dictating polymer properties[12–16].

Developing copolymer architectures beyond these conventional categories could unlock new property spaces and enable novel applications. Herein, we introduce a new class of copolymers, termed *bundle copolymers* (Fig. 1b), in which different polymer chains are aligned in parallel and covalently linked to form a multi-stranded architecture. This side-by-side arrangement contrasts with that in conventional copolymers, where monomer units are connected sequentially along a single backbone or at the chain termini. While each strand in a bundle copolymer preserves its intrinsic chemical identity, the bundled configuration is expected to profoundly influence chain dynamics and conformational behaviour, potentially giving rise to properties that are different from those of conventional copolymers. However, the realisation of this bundled architecture presents significant synthetic challenges. Unlike asymmetric rigid ladder motifs relying on specific monomer design[17–22], the parallel alignment of distinct polymer chains remains difficult and unexplored[23].

To synthesise bundle copolymers, we developed a nanoconfined polymerisation approach employing the one-dimensional (1D) nanochannels of a metal–organic framework (MOF) as a spatially confined reaction environment. MOFs provide a highly versatile platform for designing nanopores, as their size and functionality can be precisely tailored by selecting from a wide variety of metal ions and organic linkers[24–26]. While MOFs are widely recognised for their applications in catalysis[27,28], molecular capture[29,30], and separation[31,32], their use as nanoreactors for polymer synthesis has recently attracted attention[33–35]. Figure 2a presents the synthetic scheme for bundle copolymers, which capitalises on confinement within MOF nanopores. Both a polymer bearing pendant monomers (**polyA**) and free monomers (**B**) are infiltrated into 1D nanopores with diameters comparable to the thickness of the bundled polymer chains. Within these confined spaces, **polyA** adopts an axially extended conformation alongside **B**[36,37]. Under this spatial constraint, copolymerisation of the pendant monomers and **B** occurs, effectively tethering **polyA** and **polyB** chains into a bundled arrangement. Subsequent removal of the MOF scaffold yields the bundle copolymer, **polyA-*bundle*-polyB**. Importantly, this spatially guided strategy does not rely on the specific structure of the polymer species, allowing for a broad range of copolymer designs. We demonstrate the feasibility of this approach and provide structural characterisation for bundle copolymers to establish them as a new category of copolymer architecture.

Results and discussion

In this work, bundle copolymers consisting of polydimethylsiloxane (PDMS, **polyA**)[38] and vinyl polymers (**polyB**)[39,40] were synthesised (Fig. 2b). This combination of commodity polymers demonstrates the generality and practical applicability of the MOF-templated approach. Methacrylate-functionalised PDMS (**PDMS-MA**; Supplementary Figs. 1 and 2) was introduced into the nanochannels of $[In(bdc)(OH)]_n$ (**1**, bdc = 1,4-benzenedicarboxylate; Fig. 2c)[41], a MOF that features 1D hexagonal pores with diameters comparable to the thickness of double-stranded copolymers composed of PDMS and typical vinyl polymers. Infiltration of **PDMS-MA** into **1** was carried out via a solvent-assisted method[42], involving the immersion of **1** in a tetrahydrofuran (THF) solution of **PDMS-MA**, followed by slow solvent evaporation to afford a dry composite of **1** and **PDMS-MA**. The amount of **PDMS-MA** was empirically optimised to one-third of the weight of **1**, ensuring an approximate 1:1 mass ratio between **PDMS-MA** and vinyl monomers in the subsequent step. Differential scanning calorimetry (DSC) of the composite exhibited no detectable glass transition for **PDMS-MA**, indicating that the polymer chains were confined within the nanochannels and no longer retained bulk-like mobility (Supplementary Fig. 3). Successful encapsulation was further supported by intensity changes in the powder X-ray diffraction (PXRD) patterns (Supplementary Fig. 4) and a marked decrease in gas adsorption (Supplementary Fig. 5).

Following the encapsulation of **PDMS-MA** in **1**, methyl methacrylate (MMA) and a radical initiator were introduced into the nanochannels. The amount of MMA adsorbed in the composite reached 47% of the maximum loading capacity of **1**, suggesting that **PDMS-MA** occupied approximately half of the pore volume (Supplementary Fig. 6). Radical polymerisation was then initiated by heating the composite under a nitrogen atmosphere, and the conversion of MMA reached 95% (Supplementary Fig. 6). PXRD

patterns recorded before and after polymerisation confirmed that the crystallinity of **1** was retained throughout the process (Supplementary Fig. 7). The spatial arrangements and conformations of the reactants during polymerisation were evaluated by molecular dynamics simulations performed at the experimentally determined ratio of **1**, **PDMS-MA**, and MMA (Supplementary Fig. 8). Under confined conditions within the nanochannels, **PDMS-MA** adopts an extended conformation aligned along the channel axis, while MMA molecules diffuse freely within the remaining pore space without phase separation. The simulations also revealed that the pores of **1** can precisely accommodate a double-stranded **PDMS-bundle-PMMA** structure while sterically preventing the formation of an additional third polymer strand (Fig. 3a). After removal of the MOF scaffold and subsequent purification, **PDMS-bundle-PMMA** was obtained as a colourless, soluble solid. Notably, when polymerisation was performed in the absence of the MOF, the product was an insoluble, randomly crosslinked network polymer (Supplementary Fig. 9).

To confirm the formation of bundle copolymer, we conducted a comprehensive structural analysis of **PDMS-bundle-PMMA**. The ^{1}H nuclear magnetic resonance (NMR) spectrum of **PDMS-bundle-PMMA** (Fig. 3b) exhibited characteristic signals corresponding to both the PDMS and PMMA components, confirming the successful incorporation of both polymer strands. The molar ratio of PDMS to PMMA was determined from the integration ratio of these signals (PDMS/PMMA = 46/54). Broadened peaks assignable to the junction points (peaks **c** and **e**) were also observed, providing evidence for covalent linkages between the PDMS and PMMA chains. Compared with the spectrum of **PDMS-MA** (Supplementary Fig. 1), the olefinic proton signals almost completely disappeared, reflecting the efficient conversion of pendant methacrylate groups during radical polymerisation.

We then performed gel permeation chromatography (GPC) analysis to investigate the overall polymer structures. Molecular weight of the bundle copolymer was estimated relative to that of a PMMA standard, as light-scattering analysis was not applicable owing to the isorefractive property of the PDMS segment[43]. The observed molecular weight of **PDMS-bundle-PMMA** (M_n = 98,100) is significantly higher than that of the **PDMS-MA** precursor (M_n = 16,500) (Fig. 3c), indicating chain extension through radical polymerisation. To elucidate the structural features of the bundle copolymer, molecular weight of the PMMA strand was analysed after selectively degrading the PDMS chain in **PDMS-bundle-PMMA** using tetrabutylammonium fluoride (Supplementary Fig. 10)[44]. GPC analysis of the liberated PMMA revealed a molecular weight (M_n = 25,300) lower than that of **PDMS-bundle-PMMA**. Considering the molecular weights of the individual components (**PDMS-MA** precursor and PMMA strand), **PDMS-bundle-PMMA** comprises multiple PDMS and PMMA chain segments interconnected through covalent crosslinking. To visualise the morphology directly, we employed atomic force microscopy (AFM). A dilute solution of **PDMS-bundle-PMMA** was spin-cast onto a mica substrate and imaged in tapping mode[45]. As shown in Fig. 3d, flexible chain-like structures with heights comparable to those of single polymer chains were observed. This result suggests that **PDMS-bundle-PMMA** adopts a side-by-side adsorption structure on the substrate. Both molecular weight analysis and morphological observations confirmed that multiple

PDMS and PMMA chains are covalently interconnected to form a bundle copolymer, as schematically illustrated in Supplementary Fig. 11.

The hallmark of the bundle copolymer topology is the close spatial proximity of the polymer strands, arising from their parallel alignment. To experimentally validate this defining structural feature, the nuclear Overhauser effect (NOE) between the protons on PMMA and PDMS was investigated. Nuclear Overhauser effect spectroscopy (NOESY) enables the determination of internuclear distances through analysis of peak intensities, with an effective detection range of approximately 0.5 nm. Because of this short detection threshold, interchain NOE signals for polymers are typically observed only in highly aggregated environments, such as the cores of micelles and hairpin chains[46,47]. Remarkably, **PDMS-bundle-PMMA** exhibited clear interchain NOE signals between the two polymer segments. In the 1D NOESY spectrum, selective irradiation of PDMS methyl protons generated negative NOE peaks characteristic of macromolecular systems at chemical shifts corresponding to PMMA protons (Fig. 4a)[48]. This observation demonstrates that PDMS and PMMA segments are within the NOE detection range of each other. In complementary experiments, irradiation of PMMA protons yielded the corresponding NOE signals from the PDMS segment (Supplementary Fig. 12), further confirming the close spatial proximity of the two strands. In contrast, a reference block copolymer composed of PDMS and PMMA exhibited no detectable NOE signals between the polymer segments under the same measurement conditions because the distance between the chains exceeds the threshold for NOE detection (Fig. 4b). These results provide direct spectroscopic evidence that **PDMS-bundle-PMMA** adopts a tightly aligned bundled structure, distinct from those of conventional copolymers.

The synthetic strategy based on spatially confined polymerisation allows the incorporation of other monomer species without requiring significant changes to the reaction conditions. To demonstrate the generality of this method, we replaced MMA with styrene and successfully synthesised **PDMS-bundle-PS** under reaction conditions analogous to those employed for **PDMS-bundle-PMMA**. Styrene monomers were introduced into the composite preloaded with **PDMS-MA**, and radical polymerisation was conducted within the confined environment of the size-matched MOF nanopores (Fig. 5a). Polymerisation proceeded effectively without disrupting the crystallinity of the host framework, and **PDMS-bundle-PS** was obtained as a soluble polymer. Structural analyses confirmed the successful formation of a bundled architecture with a similar molar ratio of repeating units (PDMS/PS = 47/53, Fig. 5b). This was also evidenced by the shift of the GPC profile to a higher molecular weight (Fig. 5c). These results are consistent with those obtained for **PDMS-bundle-PMMA**, demonstrating the successful extension of the synthetic methodology to different monomer systems.

Considering the arrangement of polymer strands in bundle copolymers, the crosslinking density is a meaningful parameter reflecting the degree of spatial proximity between the strands. To investigate this relationship, bundle copolymers with different crosslinking densities were prepared by changing the average number of PDMS repeating units between methacrylate pendants (p). While the previously discussed samples were synthesised using **PDMS-MA** with p = 5.1, lower-density bundle copolymers were prepared from **PDMS-MA** with p = 16 (Supplementary Figs. 13–15). The resulting differences in

interchain proximity were assessed by analysing the intensities of the NOE signals under identical measurement conditions (Supplementary Fig. 16). Figure 5d shows the NOE signal intensity normalised by the compositional ratio, which provides an indication of spatial proximity to the irradiated protons[49]. The signal strength decreased with decreasing crosslinking density, suggesting an increased average interchain distance, likely due to increased conformational freedom. These results demonstrate that interstrand proximity, a key feature of bundle copolymers, can be qualitatively assessed and tuned by adjusting the crosslinking density. It should be noted that direct comparison between **PDMS-bundle-PMMA** and **PDMS-bundle-PS** is difficult because of the different chemical environments and spatial orientations of protons in the PMMA and PS units.

Finally, the thermal properties of the bundle copolymers were assessed by DSC (Supplementary Fig. 17). For comparison, conventional block copolymers (Supplementary Figs. 18–23) typically showed two clear glass transition temperatures (T_g), reflecting microphase separation[50], where each polymer component maintains its inherent mobility within separate domains. In contrast, the covalently tethered structure of the bundle copolymers resulted in thermal behaviour different from those of traditional phase-separated systems. The PDMS segment displayed broader T_g transitions, potentially due to being constrained by the more rigid vinyl polymers in the bundled architecture, which may obscure the expression of characteristic PDMS domain mobility. For the vinyl polymer components (PS and PMMA), the T_g values of the bundle copolymers were between those of the corresponding homopolymers and block copolymers. This intermediate behaviour may reflect two competing effects: (1) reduced T_g due to restricted domain size, as the polymer chains cannot form large domains in the bundled structure, and (2) elevated T_g resulting from restricted chain mobility imposed by covalent crosslinking between the strands. The vinyl polymer components in the bundle copolymers with a higher crosslinking density (p = 5.1) exhibited a less defined or higher T_g, indicating that intense interstrand proximity may fundamentally disrupt conventional polymer dynamics. This thermal behaviour suggests that the bundle topology fundamentally alters polymer chain dynamics through enforced interstrand proximity, establishing a new structural parameter that can be systematically tuned to guide future materials design.

Conclusions

We proposed bundle copolymers as a conceptually new class of copolymers, in which multiple different polymer strands are aligned in parallel and covalently connected. This unique topology provides opportunities to engineer materials with properties inaccessible to existing architectures through their defining feature—tunable interstrand spatial proximity—as demonstrated by NOE interactions. For this proof-of-concept study, we selected readily accessible commodity polymers (PDMS and PMMA/PS) to demonstrate the feasibility of the approach. Preliminary findings on the interstrand proximity and the thermal behaviour of bundle copolymers suggest potential for significant development of other properties, including viscoelastic, electrochemical, and optical properties, leveraging the highly versatile MOF-templated approach. The modular nature of this approach allows for the strategic selection of polymer components based on desired target properties, opening the way to the rational design of

bundle architectures, including multistrand, core-sheath, and woven polymers. The synthesis of **PDMS-bundle-PMMA** and **PDMS-bundle-PS** represents the first step toward establishing bundle copolymers as a promising molecular architecture for expanding the scope of macromolecular design and properties.

Methods

Synthesis of bundle copolymers

To synthesise **PDMS-bundle-PMMA**, activated **1** (1.77 g) was immersed in a solution of **PDMS-MA** (0.60 g) in THF (10 mL). The solvent was slowly evaporated at 60°C overnight to introduce **PDMS-MA** into the MOF nanochannels. The composite was further dried under vacuum to thoroughly remove residual THF from the pores. The composite of **PDMS-MA** and **1** (2.28 g) was then added to MMA (7 mL) containing benzoyl peroxide (BPO, 21 mg), and the mixture was allowed to stand at ambient temperature for 30 min. Excess MMA was removed under reduced pressure (3 kPa). After sampling a small aliquot and purging with nitrogen, radical polymerisation was carried out at 70°C for 24 h, followed by an additional 24 h at 120 ℃, yielding a composite of **1** and **PDMS-bundle-PMMA**. The MOF scaffold was removed by sequential immersion in 1 M HCl in water/MeOH (1/1), saturated $NaHCO_3$(aq), 1 M HCl in water, and 1 M EDTA·4Na in water/MeOH (1/1). The resulting product was dissolved in THF and filtered to remove MOF-derived residue. The polymer was further purified by preparative GPC to eliminate oligomeric products, affording **PDMS-bundle-PMMA** as a colourless solid. **PDMS-bundle-PS** was synthesised following the same procedure using styrene instead of MMA. Excess styrene was removed under a pressure of 0.1 kPa, and polymerisation was performed at 120°C for 24 h.

Declarations

Competing interests

The authors declare no competing interests.

Author contributions

Y. Kametani. and T.U. conceived and directed the project. Y. Kametani., Y.R., Y.A., and Y. Kawasaki. performed the experiments and analyses. Y. Kametani and T.U. wrote the manuscript with inputs from all co-authors.

Acknowledgements

This work was supported by the Japan Society for the Promotion of Science (JSPS) Grant-in-Aid for Early-Career Scientists (KAKENHI) (grant no. 23K13788), Daikin Industries, Ltd., Japan, and Japan

Science and Technology Agency (JST)-CREST (grant no. JPMJCR20T3).

References

1. Kakkar A, Traverso G, Farokhzad OC, Weissleder R, Langer R (2017) Evolution of macromolecular complexity in drug delivery systems. Nat Rev Chem 1:0063
2. Wang W, Lu W, Goodwin A, Wang H, Yin P, Kang N-G, Hong K, Mays JW (2019) Recent advances in thermoplastic elastomers from living polymerizations: Macromolecular architectures and supramolecular chemistry. Prog Polym Sci 95:1–31
3. Zhao X, Chen X, Yuk H, Lin S, Liu X, Parada G (2021) Soft materials by design: Unconventional polymer networks give extreme properties. Chem Rev 121:4309–4372
4. Saha D, Witt CL, Fatima R, Uchiyama T, Pande V, Song D-P, Fei H-F, Yavitt BM, Watkins JJ (2025) Opportunities in bottlebrush block copolymers for advanced materials. ACS Nano 19:1884–1910
5. Bareiss RE, Kahovec J, Kratochvil P (1994) Graphic representations (chemical formulas) of macromolecules (IUPAC Recommendations 1994). Pure Appl Chem 66:2469–2482
6. Corrigan N, Jung K, Moad G, Hawker CJ, Matyjaszewski K, Boyer C (2020) Reversible-deactivation radical polymerization (controlled/living radical polymerization): From discovery to materials design and applications. Prog Polym Sci 111:101311
7. Hughes RW, Lott ME, Olson RA, Sumerlin BS (2024) Photoiniferter polymerization: Illuminating the history, ascendency, and renaissance. Prog Polym Sci 156:101871
8. Harrisson S, Whitfield R, Anastasaki A, Matyjaszewski K (2025) Atom transfer radical polymerization. Nat Rev Methods Primers 5:2
9. Sheiko SS, Sun FC, Randall A, Shirvanyants D, Rubinstein M, Lee H, Matyjaszewski K (2006) Adsorption-induced scission of carbon–carbon bonds. Nature 440:191–194
10. Judzewitsch PR, Nguyen T-K, Shanmugam S, Wong EHH, Boyer C (2018) Towards sequence-controlled antimicrobial polymers: Effect of polymer block order on antimicrobial activity. Angew Chem Int Ed 57:4559–4564
11. Kametani Y, Tournilhac F, Sawamoto M, Ouchi M (2020) Unprecedented sequence control and sequence-driven properties in a series of AB-alternating copolymers consisting solely of acrylamide units. Angew Chem Int Ed 59:5193–5201
12. Dau H, Jones GR, Tsogtgerel E, Nguyen D, Keyes A, Liu Y-S, Rauf H, Ordonez E, Puchelle V, Alhan HB, Zhao C (2022) Harth, E. Linear block copolymer synthesis. Chem Rev 122:14471–14553
13. Lee H, Kwon S, Min J, Jin S-M, Hwang JH, Lee E, Lee WB, Park MJ (2024) Thermodynamically stable plumber's nightmare structures in block copolymers. Science 383:70–76
14. Maekawa S, Seshimo T, Dazai T, Sato K, Hatakeyama-Sato K, Nabae Y, Hayakawa T (2024) Chemically tailored block copolymers for highly reliable sub-10nm patterns by directed self-assembly. Nat Commun 15:5671

15. Pan M, Zhao R, Fu C, Tang M, Zhou J, Ma B, Liu J, Yang Y, Chen B, Zhang Q, Wang Y (2024) Tuning nanoparticle core composition drives orthogonal fluorescence amplification for enhanced tumour imaging. Nat Commun 15:7824
16. Sproncken CCM, Liu P, Monney J, Fall WS, Pierucci C, Scholten PBV, Van Bueren B, Penedo M, Fantner GE, Wensink HH, Steiner U, Weder C, Bruns N, Mayer M, Ianiro A (2024) Large-area, self-healing block copolymer membranes for energy conversion. Nature 630:866–871
17. Yashima E, Ousaka N, Taura D, Shimomura K, Ikai T, Maeda K (2016) Supramolecular helical systems: Helical assemblies of small molecules, foldamers, and polymers with chiral amplification and their functions. Chem Rev 116:13752–13790
18. Teo YC, Lai HWH, Xia Y (2017) Synthesis of ladder polymers: Developments, challenges, and opportunities. Chem Eur J 23:14101–14112
19. Bolgar P, Dhiman M, Núñez-Villanueva D, Hunter CA (2025) Covalent template-directed synthesis: A powerful tool for the construction of complex molecules. Chem Rev 125:1629–1657
20. Jantas R, Połowiński S (1986) Synthesis, polymerization, and copolymerization of multimethacrylate in matrix of poly(vinyl alcohol). J Polym Sci Part A: Polym Chem 24:1819–1827
21. Wu D, Sinha N, Lee J, Sutherland BP, Halaszynski NI, Tian Y, Caplan J, Zhang HV, Saven JG, Kloxin CJ, Pochan DJ (2019) Polymers with controlled assembly and rigidity made with click-functional peptide bundles. Nature 574:658–662
22. Matsuo S, Nonaka S, Mihata A, Shikinaka K, Kaneko Y (2025) Preparation and nanoaggregate formation ability in water of amphiphilic ladder-like polymers with parallelly linked hydrophilic polyether and hydrophobic polysiloxane chains. Polym Chem 16:850–857
23. Gao Y, Zhou D, Lyu J, Xu AS, Newland Q, Matyjaszewski B, Tai K, H., Wang W (2020) Complex polymer architectures through free-radical polymerization of multivinyl monomers. Nat Rev Chem 4:194–212
24. Lu W, Wei Z, Gu Z-Y, Liu T-F, Park J, Park J, Tian J, Zhang M, Zhang Q, Gentle III, Bosch T, M., Zhou H-C (2014) Tuning the structure and function of metal–organic frameworks *via* linker design. Chem Soc Rev 43:5561–5593
25. Moghadam PZ, Li A, Wiggin SB, Tao A, Maloney AGP, Wood PA, Ward SC, Fairen-Jimenez D (2017) Development of a Cambridge Structural Database subset: A collection of metal–organic frameworks for past, present, and future. Chem Mater 29:2618–2625
26. Kalmutzki MJ, Hanikel N, Yaghi OM (2018) Secondary building units as the turning point in the development of the reticular chemistry of MOFs. Sci Adv 4:eaat9180
27. Sun K, Huang Y, Sun F, Wang Q, Zhou Y, Wang J, Zhang Q, Zheng X, Fan F, Luo Y, Jiang J, Jiang H-L (2024) Dynamic structural twist in metal–organic frameworks enhances solar overall water splitting. Nat Chem 16:1638–1646
28. Panda S, Maity T, Sarkar S, Manna AK, Mondal J, Haldar R (2025) Diffusion-programmed catalysis in nanoporous material. Nat Commun 16:1231

29. Shi L, Kirlikovali KO, Chen Z, Farha OK (2024) Metal–organic frameworks for water vapor adsorption. Chem 10:484–503
30. Lin J-B, Nguyen TTT, Vaidhyanathan R, Burner J, Taylor JM, Durekova H, Akhtar F, Mah RK, Ghaffari-Nik O, Marx S, Fylstra N, Iremonger SS, Dawson KW, Sarkar P, Hovington P, Rajendran A, Woo TK, Shimizu G (2021) K. H. A scalable metal–organic framework as a durable physisorbent for carbon dioxide capture. Science 374:1464–1469
31. Hu Y, Sengupta B, Long H, Wayment LJ, Ciora R, Jin Y, Wu J, Lei Z, Friedman K, Chen H, Yu M, Zhang W (2024) Molecular recognition with resolution below 0.2 angstroms through thermoregulatory oscillations in covalent organic frameworks. Science 384:1441–1447
32. Torimoto A, Ishibashi D, Yamashita A, Uemura T, Hosono N (2025) High-precision separation and refinement of fatty acid derivatives by metal–organic frameworks. J Am Chem Soc 147:17228–17238
33. Schmidt BVK, J (2020) Metal–organic frameworks in polymer science: Polymerization catalysis, polymerization environment, and hybrid materials. Macromol Rapid Commun 41:1900333
34. Begum S, Hassan Z, Bräse S, Tsotsalas M (2020) Polymerization in MOF-confined nanospaces: Tailored architectures, functions, and applications. Langmuir 36:10657–10673
35. Nishijima A, Kametani Y, Uemura T (2022) Reciprocal regulation between MOFs and polymers. Coord Chem Rev 466:214601
36. Uemura T, Yanai N, Watanabe S, Tanaka H, Numaguchi R, Miyahara MT, Ohta Y, Nagaoka M, Kitagawa S (2010) Unveiling thermal transitions of polymers in subnanometre pores. Nat Commun 1:83
37. Uemura T, Uchida N, Asano A, Saeki A, Seki S, Tsujimoto M, Isoda S, Kitagawa S (2012) Highly photoconducting π-stacked polymer accommodated in coordination nanochannels. J Am Chem Soc 134:8360–8363
38. Yilgör E, Yilgör I (2014) Silicone-containing copolymers: Synthesis, properties and applications. Prog Polym Sci 39:1165–1195
39. Ali U, Abd Karim KJ, Bt, Buang NA (2015) A review of the properties and applications of poly(methyl methacrylate) (PMMA). Polym Rev 55:678–705
40. Singh A, Chauhan A, Gaur R (2025) A comprehensive review on the synthesis, properties, environmental impacts and chemiluminescence applications of polystyrene (PS). Discovery Chem 2:47
41. Volkringer C, Meddouri M, Loiseau T, Guillou N, Marrot J, Férey G, Haouas M, Taulelle F, Audebrand N, Latroche M (2008) The Kagomé topology of the gallium and indium metal-organic framework types with a MIL-68 structure: Synthesis, XRD, solid-state NMR characterizations, and hydrogen adsorption. Inorg Chem 47:11892–11901
42. Iizuka T, Sano H, Le Ouay B, Hosono N, Uemura T (2023) An approach to MOFaxanes by threading ultralong polymers through metal–organic framework microcrystals. Nat Commun 14:3241

43. Elkins CL, Long TE (2004) Living anionic polymerization of hexamethylcyclotrisiloxane (D_3) using functionalized initiation. Macromolecules 37:6657–6659
44. Rupasinghe B, Furgal JC (2021) Full circle recycling of polysiloxanes via room-temperature fluoride-catalyzed depolymerization to repolymerizable cyclics. ACS Appl Polym Mater 3:1828–1839
45. Abe M, Kametani Y, Uemura T (2023) Fabrication of double-stranded vinyl polymers mediated by coordination nanochannels. J Am Chem Soc 145:2448–2454
46. Voets IK, de Keizer A, Cohen Stuart MA, de Waard P (2006) Core and corona structure of mixed polymeric micelles. Macromolecules 39:5952–5955
47. Lu J, ten Brummelhuis N, Weck M (2014) Intramolecular folding of triblock copolymers *via* quadrupole interactions between poly(styrene) and poly(pentafluorostyrene) blocks. Chem Commun 50:6225–6227
48. Balaram P, Bothner-By AA, Dadok J (1972) Negative nuclear Overhauser effects as probes of macromolecular structure. J Am Chem Soc 94:4015–4017
49. Matsumoto M, Terashima T, Matsumoto K, Takenaka M, Sawamoto M (2017) Compartmentalization technologies via self-assembly and cross-linking of amphiphilic random block copolymers in water. J Am Chem Soc 139:7164–7167
50. Abdilla A, D'Ambra CA, Geng Z, Shin JJ, Czuczola M, Goldfeld DJ, Biswas S, Mecca JM, Swier S, Bekemeier TD, Laitar DS, Bates MW, Bates CM, Hawker CJ (2021) Silicone-based polymer blends: Enhancing properties through compatibilization. J Polym Sci 59:2114–2128

Figures

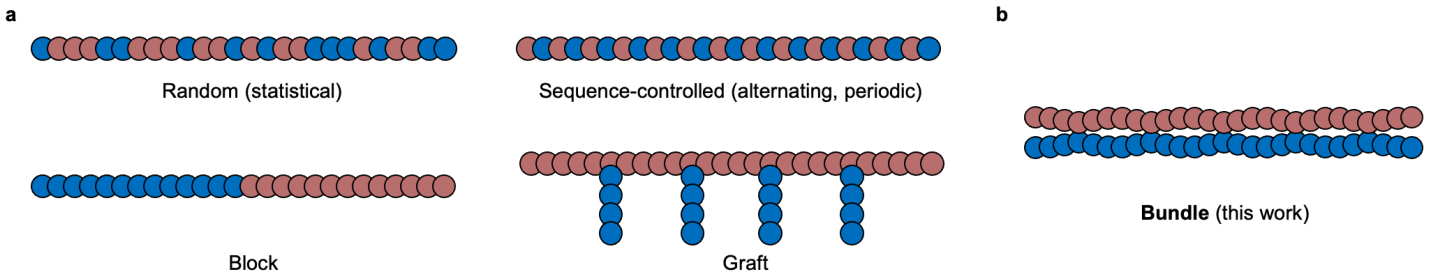

Figure 1

Concept of bundle copolymers. a, Schematic illustrations of the four conventional types of copolymers categorized by IUPAC. **b**, Schematic illustration of bundle copolymers introduced in this work. Bundle copolymers are polymers in which different polymer chains are covalently interconnected and aligned in a parallel configuration.

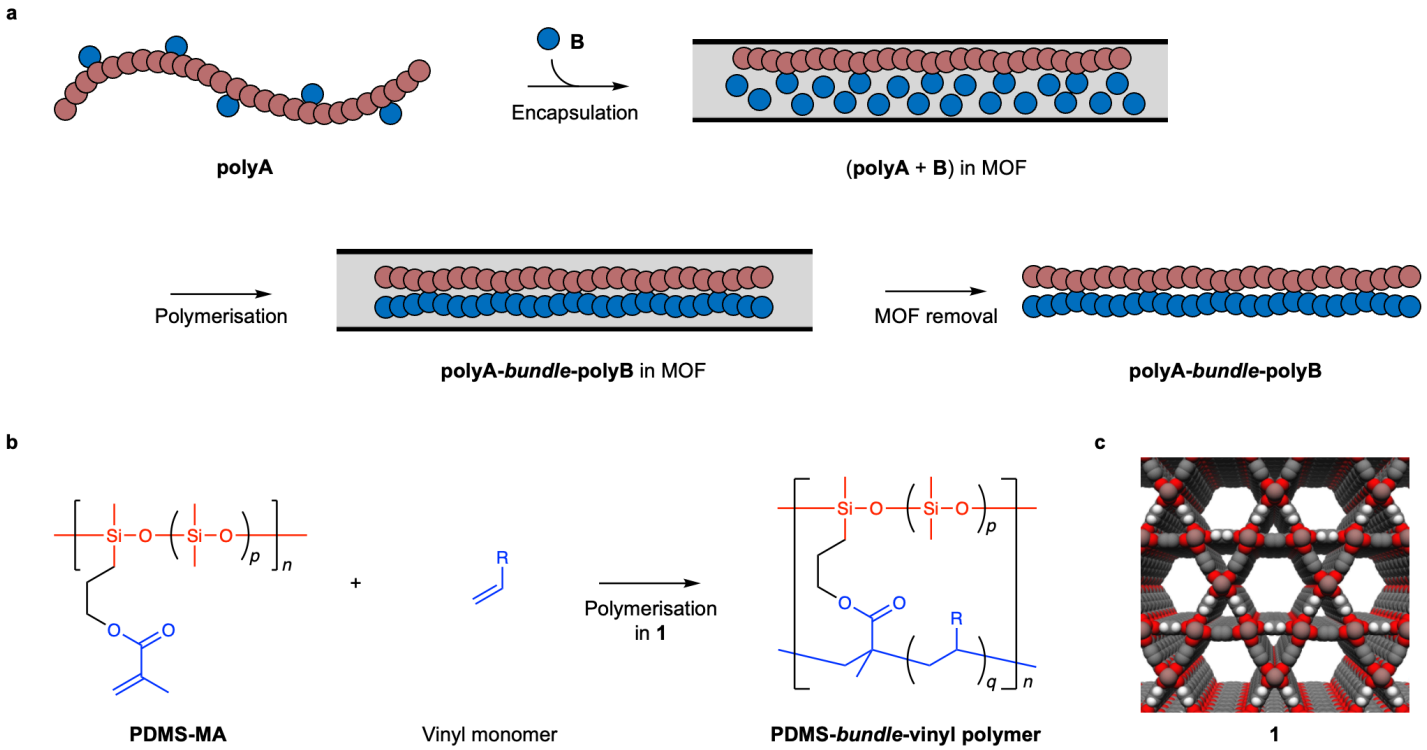

Figure 2

Synthetic approach for bundle copolymers. a, General schematic of bundle copolymer synthesis. The nanoconfined environment provided by metal–organic framework (MOF) nanochannels enables polymerisation of monomer **B** alongside polymer **A**, forming a bundled structure composed of commodity polymer strands (**polyA-*bundle*-polyB**). **b**, Scheme for **PDMS-*bundle*-vinyl polymer** via MOF-templated polymerisation. **c**, Hexagonal 1D nanochannels of **1**. The crystal structure is shown using a CPK model (In, brown; O, red; C, grey; H, white).

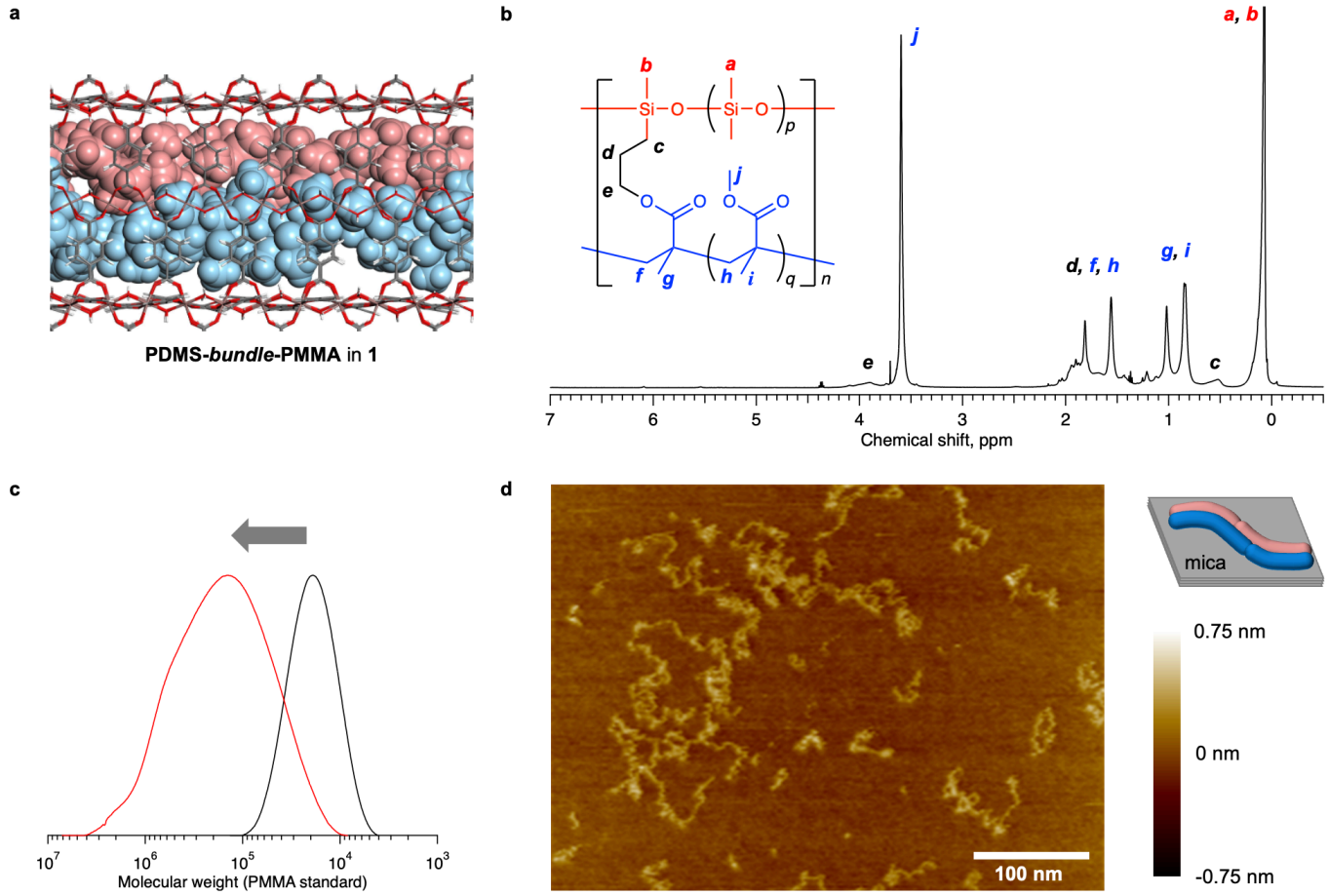

Figure 3

Characterization of PDMS-*bundle*-PMMA. a, Molecular dynamics structure of **PDMS-*bundle*-PMMA** in **1**. The polymers are shown using a CPK model (polydimethylsiloxane (PDMS), pink; poly(methyl methacrylate) (PMMA), light blue) and MOF using a stick model (In, brown; O, red; C, grey; H, white). **b**, ^{1}H NMR spectrum of **PDMS-*bundle*-PMMA** (p = 5.1) in $CDCl_3$. **c**, GPC curve of **PDMS-*bundle*-PMMA** (p = 5.1, M_n = 98,100, M_w/M_n = 3.23) (red line). The GPC curve of the **PDMS-MA** precursor (black line) is also shown for reference. **d**, AFM image of **PDMS-*bundle*-PMMA** obtained in tapping mode. A schematic representation of the polymer morphology on the substrate is also shown.

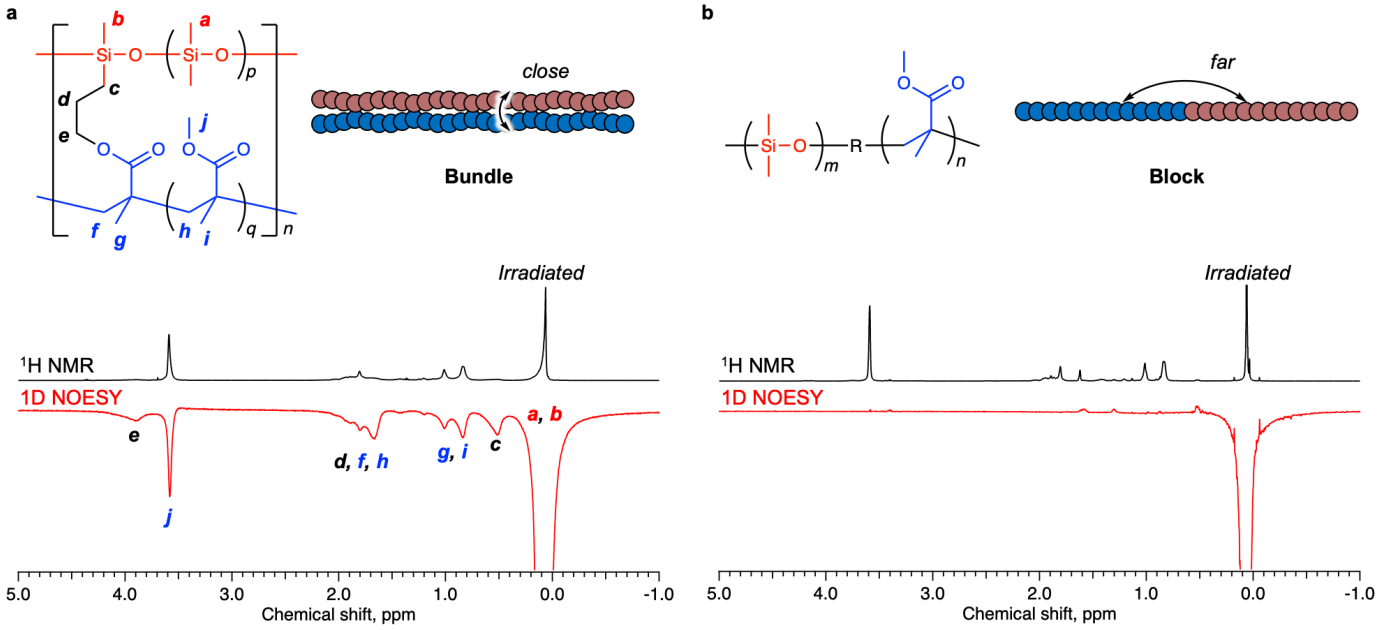

Figure 4

Evaluation of chain proximity by NOE measurements. 1D NOESY spectra of **a**, **PDMS-*bundle*-PMMA** and **b**, **PDMS-*block*-PMMA**, acquired by selective irradiation at the methyl protons of the polydimethylsiloxane (PDMS) segment (2.5% in $CDCl_3$, mixing time: 300 ms).

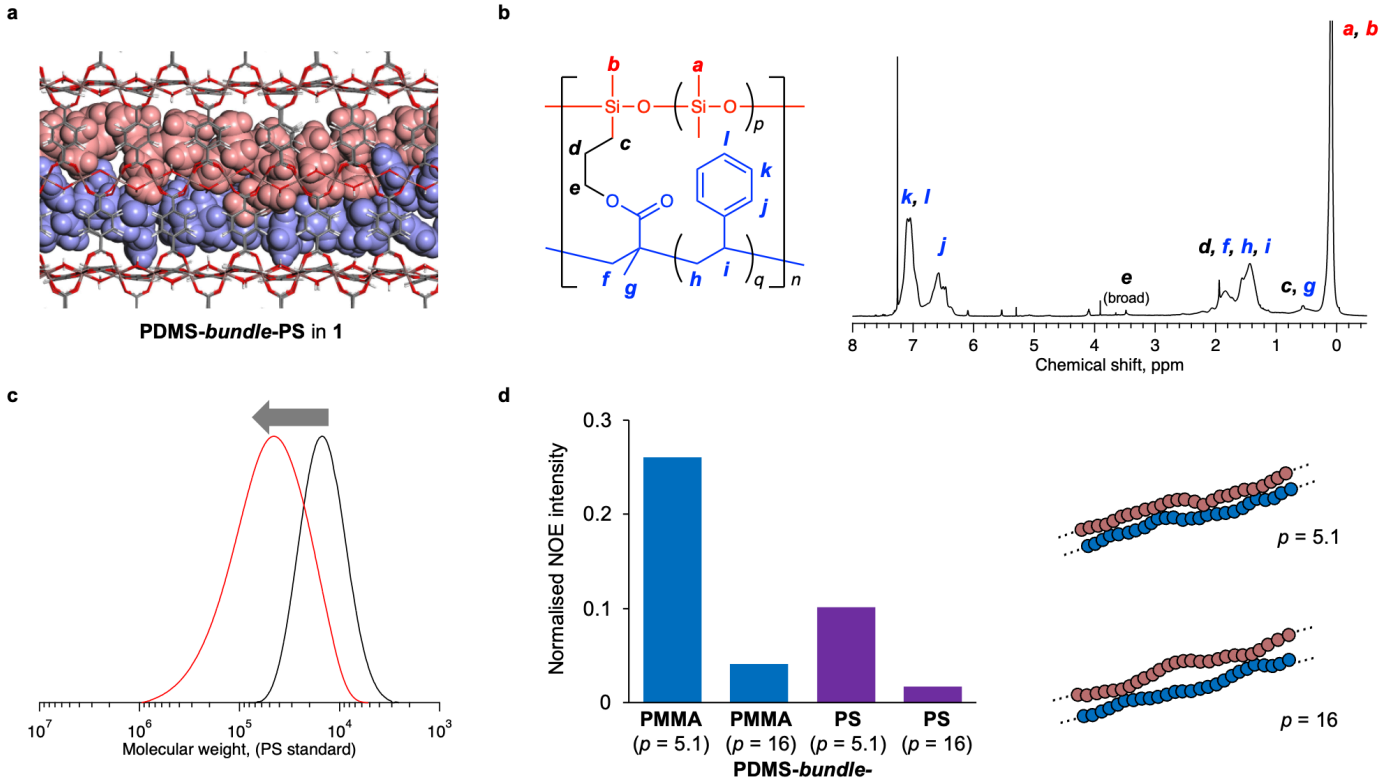

Figure 5

General applicability of the metal–organic framework (MOF)-templated approach. a, Molecular dynamics structure of **PDMS-*bundle*-PS** in **1**. The polymers are shown using a CPK model (polydimethylsiloxane (PDMS), pink; polystyrene (PS), pale purple) and MOF using a stick model (In, brown; O, red; C, grey; H, white). **b**, ^{1}H NMR spectrum of **PDMS-*bundle*-PS** (p = 5.1) in $CDCl_3$. **c**, GPC curve of **PDMS-*bundle*-PS** (p = 5.1, M_n = 37,500, M_w/M_n = 1.98) (red line). The GPC curve of the **PDMS-MA** precursor (black line) is also shown for reference. **d,** Chain proximity evaluation based on NOE intensity. Protons on the PDMS segment were irradiated, and the intensity corresponding to the protons on the vinyl polymer was measured. Details are described in Supplementary Fig. 16. A schematic representation of interchain proximity is also shown.

Supplementary Files

This is a list of supplementary files associated with this preprint. Click to download.

- SupplementaryInformation.docx